10652 *Macromolecules* **2010**, *43*, 10652–10658
DOI: 10.1021/ma102514x

Macromolecules
ARTICLE

Dispersible Shaped Nanoobjects from Bulk Microphase Separation of High T_g Block Copolymers without Chemical Cross-linking

Jianglei Qin, Yongming Chen,* Dadong Yan, and Fu Xi

*Laboratory of Polymer Physics and Chemistry, Institute of Chemistry,
The Chinese Academy of Sciences, Beijing 100190, China*

Received November 4, 2010; Revised Manuscript Received November 22, 2010

ABSTRACT: This work presents a facile procedure to fabricate the nanoobjects of block copolymers with lamellar, cylindrical, and spherical morphology via bulk microphase separation and dispersing in selective solvents without chemical cross-linking. The morphologies of these nanoobjects in solution were stabilized by their cores in a glassy state. First the bulk microphase separation of a series of poly(*tert*-butyl acrylate)-*block*-polystyrene (P*t*BA-*b*-PS) block copolymers was conducted to generate the ordered materials with lamellar, cylindrical and spherical morphology with the PS domains as the discontinuous phases as characterized by small-angle X-ray scattering (SAXS) and transmission electron microscopy (TEM). Then by direct dispersing these microphase separated materials into methanol that is a selective solvent of the P*t*BA segments, the nanoobjects, lamellae, cylinders and spheres, inherited from their bulk structures were obtained. As a contrast, micellization of these block copolymers directly in methanol all gave spherical micelles. Therefore, those nanoobjects of P*t*BA-*b*-PS via bulk microphase separation were thermodynamic unfavorable in methanol but were fixed by the glassy PS cores. Under a refluxing condition of methanol, the nanoobjects of lamellae and cylinders were transformed into spherical micelles of thermodynamic stucture as traced by TEM. It was observed that the dispersed lamellae transformed first into nanorods and then into spheres during refluxing, whereas the cylinders gradually became spheres. Furthermore, the P*t*BA segments tethered onto the glassy PS cores were hydrolyzed into the poly(acrylic acid) (PAA) segments by treating with trifluoroacetic acid, and as a result, the PAA coated nanoobjects of different morphology dispersed in the basic water were obtained without chemical cross-linking.

Introduction

Bulk self-assembly of block copolymers spontaneously produces various ordered nanostructures. Lamellar, cylindrical, and spherical morphologies are commonly formed nanostructures depending on the parameters of the polymer blocks, such as volume fraction (f), Flory−Huggins interaction parameter (χ), and degree of polymerization (N).[1,2] These nanostructures generated from block copolymers have exhibited valuable applications in nanoscience and nanotechnology, for example in preparation of dispersed nanoobjects,[3] nanocomposites,[4] and optical materials,[5] etc. Therefore, it is not surprising that synthesis and self-assembly of block copolymers have attracted much attention in recent decades.[6−10] Among these applications, preparation of dispersible polymeric nanoobjects (PNOs) first through bulk microphase separation and then fixing the uncontinuous domains and finally dispersing in a solvent of the unfixed ones has obtained increasing attention. Various dispersed nanoobjects have been prepared from the reactive block copolymers with different cross-linkable segments, such as poly(vinylpyridine),[11] polybutadiene (PB),[12−15] poly(2-cinnamoyloxyethyl methacrylate),[16−18] and poly(3-(triethoxysilyl)propyl methacrylate) (PTEPM).[19−23] Since the particle morphologies are inherited from the bulk microphase separated structures, it is easily to fabricate the nanoobjects with lamellar, cylindrical, and spherical morphologies from the same block copolymer family by changing the composition. As a contrast, in solution self-assembly of block copolymers spherical micelles are mainly obtained whereas the aggregates of different structure like vesicles, wormlike micelles and the kinetically trapped micelles are also observed but only from some block copolymers.[24−31] Therefore, bulk microphase separation approach exhibits more advantages in fabrication of the shaped PNOs from the same block copolymer family.

Recently rapid increased attention has been paid to the shape-properties relation of nanoparticles since several studies have observed that the shape does matter in biomedical functions.[32,33] Therefore, the block copolymer PNOs by chemical cross-linking with different shapes may exhibit great applications in many areas like nanomedicine for drugs delivery and tumor diagosis. It is noteworthy that these nanoobjects are of organic polymers and, therefore, they exhibt the elasticity and stimuli-responsibility, differing them greatly from the inorganic nanomaterials and organic nanocrystals. Also, these dispersed nanoobjects with controlled shape and size from block copolymer self-assembly being cross-linked have polymer brushes densely tethered from the surfaces. The hairy shells not only play a role of stabilization but also supply tremendous sites for functionalization. Moreover, the nanofabrication procedure via the bulk approach does not need solvents during self-assembly and, therefore, the products can be prepared in large scale which is more environmentally friendly. However, in order to conduct chemical fixation in the specific domains the block copolymers should have a reactive polymer segment. The reason for cross-linking is simply because that the thermodynamically stable nanostructures in bulk will become thermodynamically unstable in solution due to the interaction of solvents and polymers. Then questions were arosen: Could the shaped PNOs via bulk block copolymer microphase separation be produced without using chemical cross-linking strategy? Could simple block copolymers without

---

*Corresponding author: Y. M. Chen, email: ymchen@iccas.ac.cn.

reactive groups fulfill this purpose? These questions are very important for block copolymer applications.

It is known that polystyrene (PS) has a relatively high glass transition temperature (ca. 100 °C) and PS chains under T_g are in glassy states. PS block polymers have been applied to prepare nanoporous materials whose structures were stabilized by glassy PS domains. For examples, Hillmyer and co-workers have prepared nanoporous films with PS as continuous domains by cleavage of the polylactide (PLA) components in PS-*b*-PEO/PS-*b*-PLA polymer blends or PS−PLA block copolymers.[34,35] Xu et al. have prepared amphiphilic nanostructural thin films with PAA cylinders perpendicular to the substrate by removal of the *tert*-butyl groups of P*t*BA-*b*-PS, and the ordered PAA channels showed reversible stimuli-responsive behavior with pH and humidity.[36,37] Guo et al. have prepared nanoporous PS-*b*-PAA materials with hydrophilic pores by deprotecting P*t*BA or etching PDMS of di- and triblock copolymer in one step with HF or trifluoroacetic acid (TFA).[38] These examples indicated that PS microdomains in bulk or thin film materials are pretty stable. This property gave us a hint to fix the PNOs morphology via bulk microphase separation of the PS block copolymers at a glassy state, which should be strong enough to hold the nanostructures in a solvent. During studying the hierarchical structure of the PS-*b*-poly(4-vinylpyridine) diblock copolymers complexed with pentadecylphenol via hydrogen bonding, van Ekenstein et al have also obtained polymer cylinders by dispersing in ethanol. The block copolymer rods obtained should have been stabilized by the PS cores with high T_g. But they have not developed it into an approach of fabricating polymer nanoobjects with different morphologies.[39] When the block copolymers of PS microphase-separate in bulk and the PS becomes the discontinuous phases, dispersing the materials with ordered nanostructure in a selective solvent of another segment under a temperature below the T_g of PS should generate the PNOs with glassy PS cores. Therefore, it is possible to produce the dispersed PNOs directly in a selective solvent from the bulk microphase separated PS block copolymers without chemical cross-linking.

Scheme 1. Fabrication of Shaped Polymer Nanoobjects without Chemical Crosslinking by Bulk Microphase Separation of P*t*BA-*b*-PS Block Copolymers and Dispersing in A Selective Solvent[a]

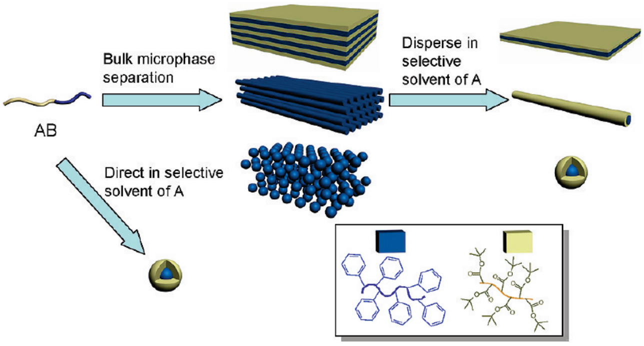

[a] The diblock copolymers of different composition may produce PNOs of the lamellae, cylinders, and spheres via bulk microphase separation whereas they only form spherical micelles via direct self-assembly in solution.

In this report, we present this simple concept for fabrication of the sovlent dispersible PNOs of different shapes from bulk microphase separation of high T_g block copolymers. Herein, the PS cores in glassy state had fixed the morphology of PNOs in a selective solvent. The P*t*BA-*b*-PS was chosen to demonstrate the concept since the P*t*BA can dissolve in methanol whereas the PS cannot. As shown in Scheme 1, the diblock copolymers with varied PS volume fraction bulk self-assembled into the materials with lamellar, cylindrical and spherical morphologies. It is noteworthy that by self-assembling directly in methanol these block copolymers only formed spherical micelles. By dispersing the P*t*BA-*b*-PS bulk materials in methanol, a selective solvent of P*t*BA, lamellae, cylinders and spheres were obtained with the P*t*BA coronas densely tethered from the frozen PS cores. Since the bulk microphase separation is thermodynamic stable, their dispersions in a good solvent of P*t*BA should be thermodynamic unstable attributing the presence of solvent−polymer corona interaction. By refluxing in methanol, these nanoobjects were transformed into uniform block copolymer spherical micelles by reorganization. Furthermore, the P*t*BA coronas were changed into the PAA by treatment of PNOs with TFA to demonstrate such nonchemically fixed nanoobjects can be surface-functionalized.

Experimental Section

Materials. Monomers *t*BA and styrene (St) were passed through a column filled with basic alumina in order to remove the inhibitor. Ethyl bromoisobutyryl bromide (EBiB) (98%, Aldrich), *N*,*N*,*N*′,*N*″,*N*″-pentamethyl diethylene triamine (PMDETA, Aldrich), and other reagents were used as received.

Synthesis of P*t*BA-*b*-PS. The bromide ended P*t*BA was first obtained by ATRP of *t*BA with EBiB as initiator at 60 °C catalyzed by CuBr/PMDETA. After purification, the P*t*BA was applied as a macroinitiator of the ATRP of St to prepare P*t*BA-*b*-PS. The polydispersity index (PDI) was determined by size exclusive chromatography (SEC) and the block ratio was characterized by ^{1}H NMR spectrum with $CDCl_3$ as solvent. Detail polymer information is listed in Table 1 in text.

Solution Self-assembly of P*t*BA-*b*-PS Copolymers. The block copolymer was dissolved in THF to give a solution of 2 mg/mL. Under vigorousl stirring, the methanol was added into the solution dropwise until the volume fraction of the methanol in the solvent was up to 80%.

Bulk Self-assembly of P*t*BA-*b*-PS Block Copolymers. The solutions of P*t*BA-*b*-PS block copolymers in THF (50 mg/mL) were spread onto Teflon plates and the solvent was evaporated slowly in THF atmosphere. The resulting bulk samples were dried for 12 h under vacuum at 45 °C. Thermal annealing was conducted at 120 °C for a week under argon to give the ordered materials with microphase separation.

Preparations of PNOs Dispersed in Methanol or Water. The self-assemblies were immersed in methanol with 1 mg/mL and stirred vigorously. After 24 h, the bulk materials disappeared and homogeneous dispersions were prepared and then the TEM investigations were performed. The hydrolysis of P*t*BA domains in the self-assemblies was carried out by stirring the bulk materials in TFA.[38] After stirring for 48 h, the resulted products were washed three times with methanol. Then the hydrolyzed self-assemblies were immersed in 1 M KOH solution and stirred vigorously for 1 h. The TEM investigations were performed after the dispersions were dialyzed against water until pH ca. 7.

Table 1. Characteristics of P*t*BA-*b*-PS Block Copolymers Synthesized in This Study

samples	M_n[a] × 10^{-3}	PDI[b]	f_{PS} (wt %)	morphology	*d*-spacing (nm)[c]
P*t*BA$_{141}$-*b*-PS$_{147}$	33.3	1.08	45.9	lamella	28.3
P*t*BA$_{310}$-*b*-PS$_{189}$	59.3	1.10	33.1	cylinder	35.9
P*t*BA$_{310}$-*b*-PS$_{90}$	49.0	1.10	19.1	sphere	25.6

[a] Calculated according to ^{1}H NMR. [b] Determined by GPC with PS standard. [c] Determined by SAXS.

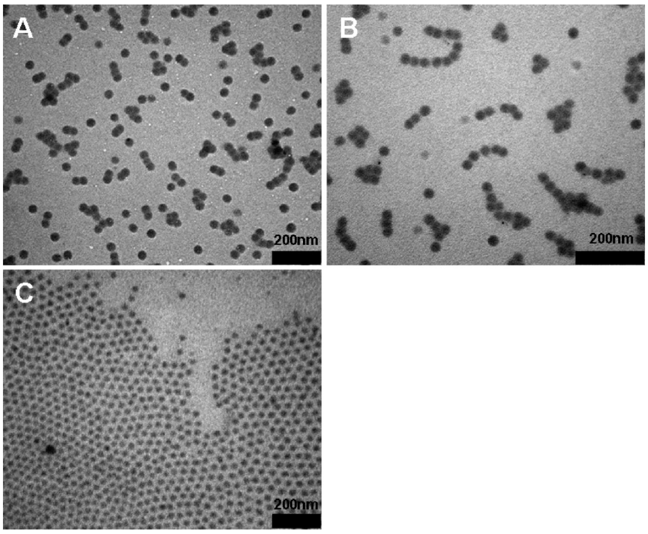

Figure 1. TEM images of solvent self-assemblies prepared from (A) P*t*BA$_{141}$-*b*-PS$_{147}$, (B) P*t*BA$_{310}$-*b*-PS$_{189}$, and (C) P*t*BA$_{310}$-*b*-PS$_{90}$.

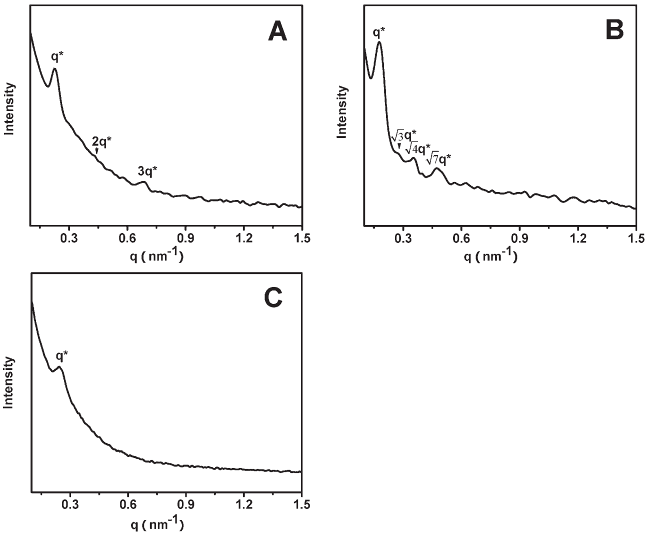

Figure 2. SAXS curves of bulk self-assembly prepared from (A) P*t*BA$_{141}$-*b*-PS$_{147}$, (2) P*t*BA$_{310}$-*b*-PS$_{189}$, and (C) P*t*BA$_{310}$-*b*-PS$_{90}$.

Morphological Transformation of the PNOs. The methanol for dispersing nanoobjects was brought to refluxing at the boiling point of methanol (65 °C). The TEM investigations were performed at predetermined intervals to trace the transforming process.

Characterization. Size exclusive chromatography (SEC) was performed on a set of Styragel columns equipped with a Waters 515 HPLC pump and a Waters 2414 refractive index detector. THF was used as eluent with a flow rate of 1.0 mL/min at 35 °C and polystyrene standards were used for calibration. ^{1}H NMR spectra were recorded on a Bruker AV400 spectrometer with CDCl$_3$ as solvent at room temperature. Fourier-transform infrared (FT-IR) spectroscopy was recorded by a Thermo Nicolet Avatar330 spectrometer, and samples were prepared by solvent casting on a KBr plate. Transmission electron microscopy (TEM) images were obtained on a Hitachi H-800 instrument operated at an accelerating voltage of 100 kV. The images were recorded by a digital camera and the samples were dropped onto carbon-coated grids for TEM observation. The microtomed slices of bulk block copolymers were stained by ruthenium tetroxide vapor before analysis. Small-angle X-ray scattering (SAXS) experiments were performed on a SAXS system, Rigaku RU300, with copper rotating anode (λ = 1.54 Å) operated at 40 kV and 50 mA.

Results and Discussion

P*t*BA-*b*-PS Block Copolymers: Synthesis and Self-Assembly in Solution. The block copolymers were prepared by the sequent ATRP of *t*BA and St, respectively. The SEC evolution of P*t*BA and P*t*BA-*b*-PS showed that the P*t*BA initiated PS successfully and gave the products with a low PDI, as shown in Figure S1 and Figure S2 (in the Supporting Information). The degree of polymerization of the P*t*BA block was evaluated by monomer conversion. The block ratios were calculated by comparing the proton peak areas of two segments from ^{1}H NMR spectrum (Figure S3 in the Supporting Information). The degree of polymerization, molecular weights and composition of block copolymers were thus obtained. Three P*t*BA-*b*-PS block copolymers with different PS weight fractions are listed in Table 1. The weight fractions of PS (f_{PS}) were changed from 45.1 wt %, 33.1 to 19.1 wt %.

Before studying their bulk nanostructures and preparing PNOs, the self-assembly of three block copolymers in a selective solvent of P*t*BA segments was conducted to examine their micellar morphologies in solution for comparison. When methanol was added into the THF solutions of three block copolymers (volume fraction of methanol was 80%), blue tint solutions were obtained and their TEM images (Figure 1) demonstrate that three samples self-assembled into core/shell spherical micelles with uniform diameters no matter the PS volume fraction of the samples. The average diameters of the dark cores of these micelles of P*t*BA$_{141}$-*b*-PS$_{147}$ (Figure 1A), P*t*BA$_{310}$-*b*-PS$_{189}$ (Figure 1B) and P*t*BA$_{310}$-*b*-PS$_{90}$ (Figure 1C) were 41, 32, and 27 nm, respectively. It would be interesting to see if these block copolymers may form the nonspherical PNOs in menthanol dispersion via bulk self-assembly.

Bulk Self-Assembly of P*t*BA-*b*-PS Block Copolymers and Formation of Shaped PNOs in Methanol. The bulk materials were prepared by casting the THF solutions of P*t*BA-*b*-PS block copolymers onto Teflon plates to form the films which were then annealed. A series of ordered nanomaterials with lamellar, cylindrical and spherical morphologies from P*t*BA-*b*-PS block copolymers were obtained as characterized by SAXS illustrated in Figure 2. The SAXS curve of the self-assembly of P*t*BA$_{141}$-*b*-PS$_{147}$ with f_{PS} of 45.1 wt % is shown in Figure 2A and a lamellar morphology with the peak pattern of 1:2:3 was obtained. The *d*-spacing was calculated from the primary peak at low *q*, and the value was 28.3 nm. For the block copolymer of P*t*BA$_{310}$-*b*-PS$_{189}$, whose f_{PS} was 33.1 wt %, the SAXS curve in Figure 2B illustrated a series of peaks with the peak position of 1:$\sqrt{3}$:$\sqrt{4}$:$\sqrt{7}$, consistent with a hexagonally packed cylindrical structure. From the primary peak position value at low *q*, the average *d*-spacing was calculated to be 35.9 nm. As for P*t*BA$_{310}$-*b*-PS$_{90}$ with f_{PS} = 19.1 wt %, Figure 2C gave a SAXS curve, whose feature was consistent with a liquid-like packing of spheres with an average *d*-spacing of 25.6 nm. The microphase separated structures were also analyzed by TEM of the microtomed slices from three samples. As shown in parts A and B of Figure S4 (Supporting Information), the patterned lamellae and cylinders were observed whereas less ordered spheres were found, further proving the structures. The properties of the microphase structure were collected into Table 1.

Since methanol is a selective solvent of P*t*BA but a poor solvent for PS, it could dissolve the P*t*BA segments while the PS cores should be kept intact. Under the temperature lower than T_g of PS, the frozen PS cores were expected to keep the nanostructure in solutions to produce the well-defined

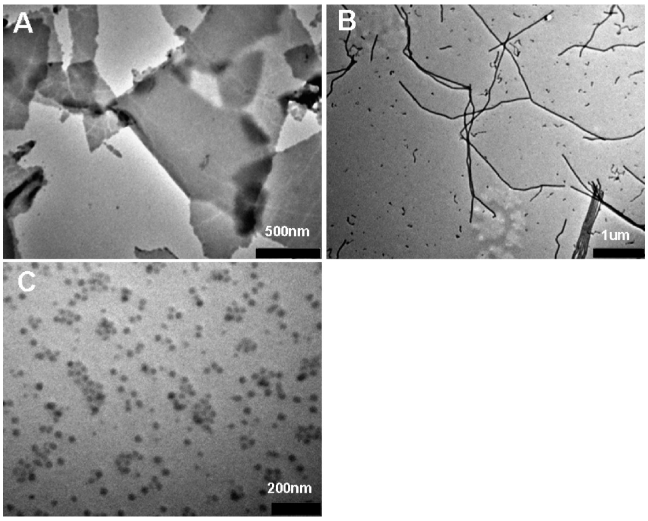

Figure 3. TEM images of methanol dispersed nanoojects prepared from bulk self-assemblies of (A) P*t*BA$_{141}$-*b*-PS$_{147}$, (B) P*t*BA$_{310}$-*b*-PS$_{189}$, and (C) P*t*BA$_{310}$-*b*-PS$_{90}$.

nanoobjects with different shapes. After stirred in methanol at room temperature for 24 h, the bulk materials disappeared and homogeneous dispersions were prepared. As for the appearance, the dispersion prepared from P*t*BA$_{141}$-*b*-PS$_{147}$ looked translucent, indicating larger size of the nanoobjects. The TEM image of the methanol dispersed nanoobjects from bulk P*t*BA$_{141}$-*b*-PS$_{147}$ (Figure 3A) demonstrated lamellae with a uniform thickness and clear edges. As for P*t*BA$_{310}$-*b*-PS$_{189}$, the dispersion became transparent, and a blue tint implied small and uniform size of the PNOs. As shown in Figure 3B, cylinders with an average diameter of 33 nm were obtained by dispersing the P*t*BA$_{310}$-*b*-PS$_{189}$ bulk. Length of the cylinders reached several micrometers; but short rods were coexisted. It is noteworthy that the cylinders looked rigid and there were inflection points along straight cylinders. This was a hint that the glassy PS cores should be stiff and brittle. The last sample from the P*t*BA$_{310}$-*b*-PS$_{90}$ self-assembly gave a clear solution. Figure 3C showed the TEM image of its dispersed particles, and the uniform spheres with a diameter of around 30 nm were illustrated. These three morphologies in methanol dispersion agreed well with the structures in bulk, demonstrating that the bulk morphology was transferred into the solution dispersion without cross-linking. Therefore, these shaped nanoobjects should be stabilized by the glassy PS cores from which the P*t*BA segments were densely tethered for solvation in methanol. Thus, well-defined PNOs without applying chemical cross-linking strategy were obtained by dispersing the bulk self-assemblies in the selective solvent at mild temperature.

The above observed dispersed shaped nanoobjects in methanol were contrasted with the results of direct solution self-assembly which gave spherical micelles exclusively from these three block copolymers. Thus, it is very interesting that the block copolymers that form spherical micelles in solution may be swithed into nonspherical PNOs but via an indirect procedure of bulk microphase separation and dispersion. The glassy cores behave like a “chemical cross-linking”, which is much facile to fix the morphologies of nanoobjects. The difference indicates that the shaped PNOs like lamellae and cylinders via the bulk approach should be the kinetically trapped structures which are thermodynamically unstable in methanol.

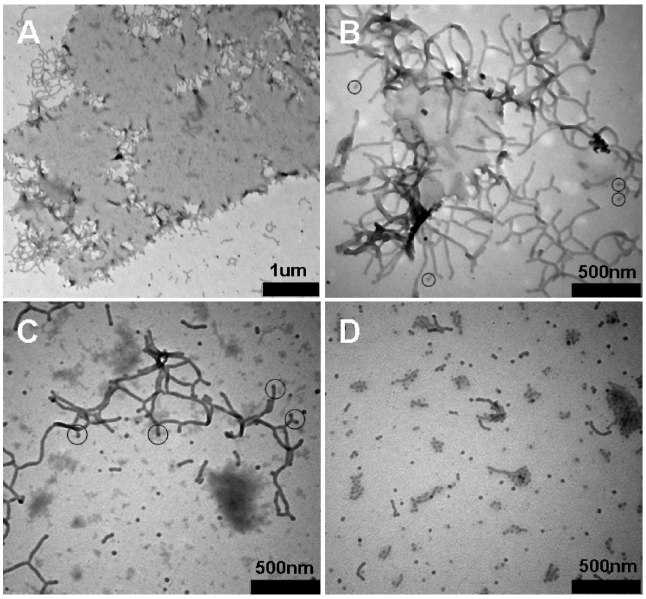

Figure 4. Morphology evolution of the lamellae in refluxing methanol for (A) 2, (B) 5, (C) 10, and (D) 24 h.

Morphological Transformation of the Nanoobjects in Refluxed Methanol. It is known that the T_g of the bulk PS is of ca. 100 °C and it may be decreased obviously by reducing the film thickness to nanosize.[40,41] Since the nanoobjects were dispersed in menthanol, we considered whether the refluxing temperature of menthanol (65 °C) was high enough to destroy the glassy PS cores in a thickness of 20−30 nm for this special case. If the PS chains in the cores become movable, the structures of the nanoobjects should change and reassemble to the structure that is in a thermodynamic equilibrium.

Three dispersed PNOs in refluxing methanol were investigated by TEM at predetermined intervals. Other than the nanospheres, both the dispersed lamellae and cylinders had been transformed into spheres with a uniform diameter by refluxing treatment. It was very interesting to observe that the lamellae from P*t*BA$_{141}$-*b*-PS$_{147}$ were transformed into nanospheres through a nanorod intergradation as shown in Figure 4. At 2 h of refluxing the nanorods with diameter of 38 nm began to form at the edges of the plates as displayed in Figure 4A. After 5 h, most parts of the lamellae had been transformed into nanorods, some with branches (Figure 4B). Note the semispheres at the ends of the nanorod marked, which seems to be split as the spheres. Further refluxed for 10 h, the dispersion turned more transparent; the lamellae disappeared and the coexisted nanorods and nanospheres with both diameters of around 38 nm were observed from Figure 4C. Only a few short rods existed whereas the majority became spheres after refluxed for 24 h (Figure 4D) and the spheres were observed exclusively after 48 h (Figure S5 in Supporting Information). The size of spheres is almost the same as the spherical micelles from the solution self-assembly of P*t*BA$_{141}$-*b*-PS$_{147}$, indicating that the transition product is core/shell micelles.

The cylinders from P*t*BA$_{310}$-*b*-PS$_{189}$ transformed into nanospheres directly by spliting the cylinders from the semispherical ends. After refluxing for 10 h, the cylinders were shortened greatly and some spheres with an average diameter of 33 nm were coexisted (Figure 5A). After 24 h, most of the cylinders had transformed into nanospheres (Fgiure 5B). The size of resulting nanospheres was comparable to that of the spherical micelles in solution self-assemblies. Above results have confirmed that the PNOs through the bulk approach are thermodynamically unstable in methanol under mild temperature and they may be transformed into their thermodynamic structures

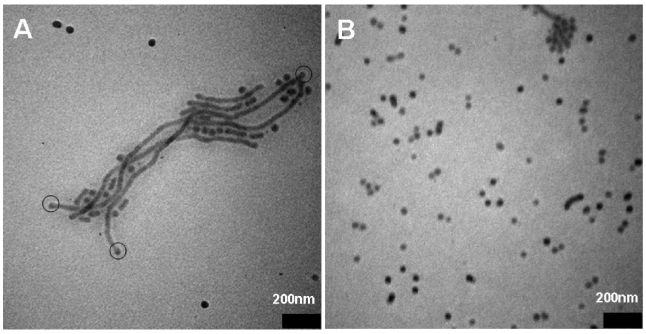

Figure 5. Morphology evolution of the cylinders to the spheres in refluxing methanol for (A) 10 and (B) 24 h.

when the temperature is increased. We had also checked if there was ester exchange reaction between methanol and the *t*Bu groups of the polyacrylate segments during refluxing by using P*t*BA$_{90}$ in methanol solution. The result of ^{1}H NMR spectrum (Figure S6 in the Supporting Information) showed negligible side reaction after 24 h. Therefore, we believed that the temperature change is the main factor to induce the morphology transformation.

Discussion. For a given AB diblock copolymer, f becomes the main factor to determine structures of the bulk microphase separation. When f_A is comparable to f_B, i.e., the symmetric block copolymers, the AB diblock copolymers form lamellae. With increase of f_A, the interfacial curvature of A and B domains increases and the microphase structure developes into cylinders and spheres with the B domains become the discontinuous phases. However, in solution self-assembly of AB diblock copolymers, supposed in a selective solvent of A, the solvent-corona A interaction plays an important role and the AB diblock copolymers form spherical micelles in a large region of f. In order to decrease the interfacial curvature to form cylindrical micelles and bilayer vesicles, f_B of the core forming segment should be much larger than f_A, namely highly asymmetric block copolymers are needed. For example, Eisenberg et al have reported that in selective solvents highly asymmetric block copolymers PS-*b*-poly(acrylic acid) or PS-*b*-poly(ethylene oxide) form aggregates of varioues morphologies.[27,28,42] With decrease of PAA segments in PS-*b*-PAA (or PEO in PS-*b*-PEO), spherical micelles transformed first into wormlike micelles and then into bilayer vesicles. To form the cylinders and vesicles, the fraction of PAA (or PEO) segments should be as low as ca. 10%, in order to respond the decrease of corona chain repulsion.

In the present work, the bulk microphase separation of P*t*BA-*b*-PS samples gave three different thermodynamic stable structures. Also the exclusively spherical micelles by direct solution self-assembly from three block copolymers are thermodynamic stable. However, we have obtained lamellar and cylindrical PNOs from the samples P*t*BA$_{141}$-*b*-PS$_{147}$ and P*t*BA$_{310}$-*b*-PS$_{189}$ via a procedure of first bulk self-assembly and then dispersing in the solvent of P*t*BA. The reason can be explained easily. When the bulk samples were dispersed in methanol, the solvent molecules only dissolved the P*t*BA phases whileas the high T_g PS cores remained intact and, as a result, dispersible lamellar and cylindrical PNOs were produced. It is obvious that the corona should have been highly solvated and the neighboring P*t*BAs should exhibit strong repulsion, resulting a strong tension to induce the interfacial curvature between core/corona to occur morphological transformation. However, due to the frozen PS cores in which the mobility of PS chains was extremely low, reorganization of block copolymer chains was nearly impossible. Therefore, the nonspherical structures in methanol stabilized by the frozed PS cores were obtained although they were energetic unfavorable.

Then it was expected that these shaped aggregates in methanol would transfer into the stable spherical micelles when the temperature was increased to the T_g of the PS cores or the plasticizers were presented. Herein, we treated these nonspherical PNOs in refluxing temperature of methanol and had observed the transformation process from the unstable structure into the stable structure. With time of refluxing, the cylinders developed exclusively into spherical micelles. During this process, the curvature tension was released by morphology transforming. However, instead of changing into the spherical particles directly, the lamellae first changed to the nanorods and then to the spheres. The reason can be understood from the phase diagram,[43] in which when temperature is increased (with the fixed polymer composition), the system undergoes a path from lamellar phase to cylindrical phase, and then to spherical phase. The real dynamic process also takes a similar path, in which the system starts from the initial unstable lamellar phase and evolves to the final stable spherical phase. The metastable (transitional) phases can be found on this path. On the other hand, from the viewpoint of energy, this multistep process costs lower energy comparing with one-step process from the lamellar phase to spherical phase directly. In terms of treating bulk spheres in methanol, it seems that no noticeable change was observed. But it is understandable that the spheres via bulk differ to the spherical micelles by direct solution approach if the thermodynamic difference was considered.

Morphology changing to the energetic favorable structure has demonstrated that the refluxing condition had softened the PS cores to allow the polymer chains to move. Since the thickness of PS cores was ca. 30 nm and the T_g of PS in this size could be much lower than that of bulk PS materials,[40,41] the refluxing temperature of methanol should close to the T_g of PS cores of these shaped nanoobjects. Another factor, plasticizing the PS cores by penetrating methanol molecules, might also contribute the transformation, but to make an evaluation on its extent to decrease the T_g of PS is beyond the focus of this paper.

The finding in this research is important for application of block copolymer self-assembly to generate the PNOs with different morphologies. In general, the block copolymers to form nonspherical self-assemblies, typically cylinders, by direct self-assembly in solution are highly asymmetric in composition. During practice it was found that some block copolymers like PS-*b*-PAA, PS-*b*-PEO, or PB-*b*-PEO may form wormlike micelles and vesicles.[24−28] However, it does not mean that any asymmetric amphiphilic block copolymers can form these cylinders. Present work supplies a general approach to fabricate nonspherical PNOs provided one component exhibits high T_g. Furthermore, relative to the solution self-assembly, the ordered structures are formed in bulk and no solvents are needed. Also relative to the bulk chemical cross-linking, this approach does not need reactive block copolymers and cross-linking strategies. All these characteristics have endowed this approach with many advantages.

Hydrolysis to Give Water Dispersed PNOs. As the P*t*BAs can be hydrolyzed into the PAAs with pH responsibility, we have transformed these PNOs into water media. After hydrolyzed and dispersed in basic water, the water dispersed nanoobjects were investigated with TEM and the images are shown in Figure 6. The nanoobjects hydrolyzed from

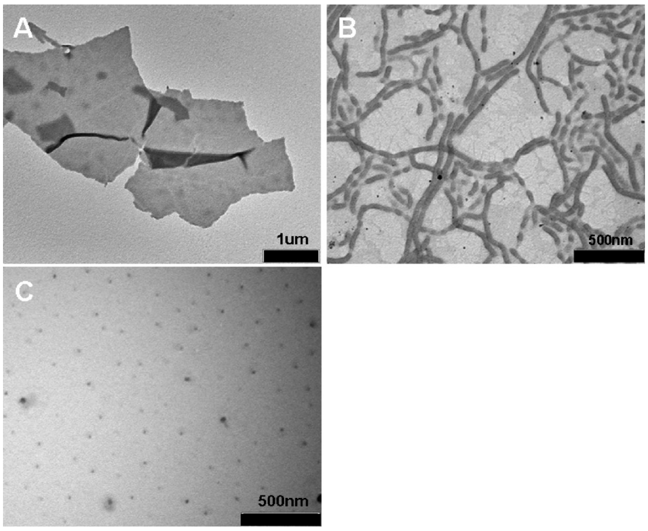

Figure 6. TEM images of water dispersed nanooject of PAA-*b*-PS by hydrolysis of the bulk self-assemblies of (A) P*t*BA$_{141}$-*b*-PS$_{147}$, (B) P*t*BA$_{310}$-*b*-PS$_{189}$, and (C) P*t*BA$_{310}$-*b*-PS$_{90}$ respectively.

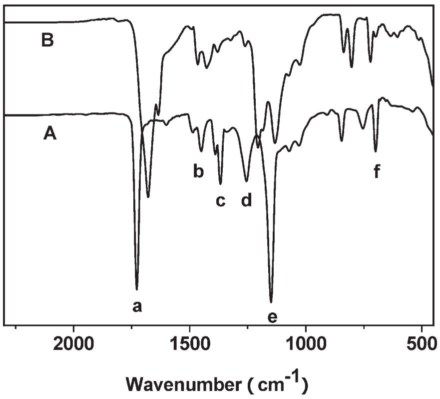

Figure 7. FT-IR spectra of the cylinders of P*t*BA$_{310}$-*b*-PS$_{189}$ (A) before and (B) after hydrolysis. (a) C═O (ester) stretching at 1730 cm^{-1}, (b) C−H stretching (1489, 1454 cm^{-1}) in monosubstituted phenyl group, (c) −CH$_3$ bending (1394, 1368 cm^{-1}) in *t*Bu group, (d) C−C−O stretching (1259 cm^{-1}) in O-*t*Bu group, (e) C−O stretching (1151 cm^{-1}) in O−*t*Bu group and (f) monosubstituted phenyl group at 700 cm^{-1}.

P*t*BA$_{141}$-*b*-PS$_{147}$ bulk self-assembly remained as lamellae (Figure 6A). Similarly, water dispersible cylinders (Figure 6B) and nanospheres (Figure 6C) were obtained by hydrolysis of P*t*BA$_{310}$-*b*-PS$_{189}$ and P*t*BA$_{310}$-*b*-PS$_{90}$ self-assemblies, respectively. The results indicated that the hydrolysis would not destroy the preformed PS microdomains, implying the PS glassy cores were pretty robust. Detailed hydrolytic efficiency of the P*t*BA domains was characterized with FT-IR spectra. As an example, and the FT-IR spectra of methanol and water dispersed cylinders prepared from P*t*BA$_{310}$-*b*-PS$_{189}$ were illustrated in Figure 7. C−CH$_3$ bending (*t*Bu) at 1394 and 1368 cm^{-1}, C−C−O stretching (O-*t*Bu) at 1259 cm^{-1} and C−O stretching from O-*t*Bu at 1151 cm^{-1} in Figure 7A represented the *t*Bu groups in the self-assembly. After hydrolyzed for 48 h in TFA, the characteristic peaks from *t*Bu groups disappeared almost completely as shown in Figure 7B. The peak at 1730 cm^{-1} corresponding to the ester carbonyl group shifted to 1680 cm^{-1} and was broadened with a shoulder at 1630 cm^{-1}. At this stage, the carboxylic ions were formed due to the pK_a of PAA was 4.7. This result indicated that the present PNOs can be modified and functionalized, which is meaningful for their application.

As the PAA was pH-responsive, the dispersibility of the nanoobjects was mediated by pH and the water dispersed lamellae was applied to check the pH-responsibility. When the pH was changed to 3, the lamellae precipitated from the dispersion to the bottom of the bottle in few minutes. When the pH was changed to 10, the sediments disappeared and the lamellae became dispersed again with same appearance as that before the pH cycle (Figure S7 in the Supporting Information). The TEM investigation was performed after the pH was dialyzed to 7, and the morphology of the isolated lamellae was remained (Figure S8 in the Supporting Information).

Conclusion

We reported a facile approach to generate the dispersible PNOs with different morphology by bulk self-assembly of P*t*BA-*b*-PS block copolymers without chemical cross-linking followed by dispersing in a solvent. The key factors are the PS with high T_g and the selective solvent of P*t*BA in dispersion. Then the frozen PS cores may stabilize the shapes of the dispersed nanoobjects. The morphological transformation was observed when the PNOs from bulk microphase separation were heated in methanol, indicating that they were energetic unfavorable in a solvent of P*t*BA. Moreover, the tethered P*t*BA segments in highly density can be swithed into the functionalized PAA corona. Still the nanoobjects remained their shapes and also exhibited pH sensitivity. This approach provides a novel but simple method to prepare the PNOs of blocks copolymers, which are very useful for nanomaterials and nanotechnology. Furthermore, the cylinders and sheets have glassy PS cores which are rigid and stiff but may be softened under certain conditions. This property may be meaningful for manipulation of single nanoobjects. Since no chemical cross-linking, these shaped PNOs may deassemble easily in solution when common solvents are introduced.

Acknowledgment. Financial support from the National Natural Science Foundation of China (50973119 and 20625412) is gratefully acknowledged.

Supporting Information Available: Figure S1−S8 showing the SEC traces of the block copolymerization, the ^{1}H NMR spectrum of P*t*BA$_{141}$-*b*-PS$_{147}$, TEM images of microtomed slices of three bulk samples and of spherical particles after 48 h reflux of P*t*BA$_{141}$-*b*-PS$_{147}$, ^{1}H NMR spectra to clarify minor ester exchange of P*t*BA, pH responsibility of water dispersed lamellae and its TEM image. This material is available free of charge via the Internet at http://pubs.acs.org.

References and Notes

(1) Bates, F. S.; Fredrickson, G. H. *Annu. Rev. Phys. Chem.* **1990**, *41*, 525–557.
(2) Hamley, I. W. *The Physics of Block Copolymers*; Oxford University Press: New York, 1998.
(3) Simon, P. F. W.; Ulrich, R.; Spiess, H. W.; Wiesner, U. *Chem. Mater.* **2001**, *13*, 3464–3486.
(4) Haryono, A.; Binder, W. H. *Small* **2006**, *2*, 600–611.
(5) Kang, C.; Kim, E.; Baek, H.; Hwang, K.; Kwak, D.; Kang, Y.; Thomas, E. L. *J. Am. Chem. Soc.* **2009**, *131*, 7538–7539.
(6) Fasolka, M. J.; Mayes, A. M. *Annu. Rev. Mater. Res.* **2001**, *31*, 323–355.
(7) Liu, T.; Burger, C.; Chu, B. *Prog. Polym. Sci.* **2003**, *28*, 5–26.
(8) Hillmyer, M. A. *Adv. Polym. Sci.* **2005**, *190*, 137–181.
(9) Ma, M. l.; Titievsky, K.; Thomas, E. L.; Rutledge, G. C. *Nano Lett.* **2009**, *9*, 1678–1683.
(10) Gao, L. C.; Yao, J.; Shen, Z. H.; Wu, Y. X.; Chen, X. F.; Fan, X. H.; Zhou, Q. F. *Macromolecules* **2009**, *42*, 1047–1050.
(11) Ishizu, K.; Fukutomi, T. *J. Polym. Sci., Part C: Polym. Lett.* **1988**, *26*, 281–286.
(12) Erhardt, R.; Böker, A.; Zettl, H.; Kaya, H.; Pyckhout-Hintzen, W.; Krausch, G.; Abetz, V.; Müller, A. H. E. *Macromolecules* **2001**, *34*, 1069–1075.

(13) Walther, A.; Drechsler, M.; Müller, A. H. E. *Soft Matter* **2009**, *5*, 385–390.

(14) Yelamanchili, R. S.; Walther, A.; Müller, A. H. E.; Breu, J. *Chem. Commun.* **2008**, *9*, 489–492.

(15) Schacher, F.; Yuan, J. Y.; Schoberth, H. G.; Müller, A. H. E. *Polymer* **2010**, *51*, 2021–2032.

(16) Yan, X. H.; Liu, G. J.; Liu, F. T.; Tang, B. Z.; Peng, H.; Pakhomov, A. B.; Wong, C. Y. *Angew. Chem., Int. Ed.* **2001**, *40*, 3593–3596.

(17) Yan, X. H.; Liu, F. T.; Li, Z.; Liu, G. J. *Macromolecules* **2001**, *34*, 9112–9116.

(18) Yan, X. H.; Liu, G. J.; Li, Z. *J. Am. Chem. Soc.* **2004**, *126*, 10059–10062.

(19) Zhang, K.; Gao, L.; Chen, Y. M. *Macromolecules* **2007**, *40*, 5916–5922.

(20) Zhang, K.; Gao, L.; Chen, Y. M.; Yang, Z. Z. *Chem. Mater.* **2008**, *20*, 23–25.

(21) Zhang, K.; Gao, L.; Chen, Y. M. *Macromolecules* **2008**, *41*, 1800–1807.

(22) Zhang, K.; Gao, L.; Zhang, C.; Chen, Y. M. *J. Mater. Chem.* **2009**, *19*, 3482–3489.

(23) Zhang, K.; Gao, L.; Zhang, C.; Chen, Y. M. *Polymer* **2010**, *51*, 2809–2817.

(24) Won, Y. Y.; Davis, H. T.; Bates, F. S. *Science* **1999**, *283*, 960–963.

(25) Lee, J. C. M.; Bermudez, H.; Discher, B. M.; Sheehan, M. A.; Won, Y. Y.; Bates, F. S.; Discher, D. E. *Biotechnol. Bioeng.* **2001**, *73*, 135–145.

(26) Jain, S.; Bates, F. S. *Science* **2003**, *300*, 460–464.

(27) Zhang, L. F.; Eisenberg, A. *Science* **1999**, *268*, 1728–1731.

(28) Desbaumes, L.; Eisenberg, A. *Langmuir* **1999**, *15*, 36–38.

(29) Gaedt, T.; Ieong, N. S.; Cambridge, G.; Winnik, M. A.; Manners, I. *Nat. Mater.* **2009**, *8*, 144–150.

(30) Qian, J. S.; Zhang, M.; Manners, I.; Winnik, M. A. *Trends Biotechnol.* **2009**, *28*, 84–92.

(31) Gilroy, J. B.; Gädt, T.; Whittell, G. R.; Chabanne, L.; Mitchels, J. M.; Richardson, Robert. M.; Winnik, M. A.; Manners, I. *Nature Chem.* **2010**, *2*, 566–570.

(32) Geng, Y.; Dalhaimer, P.; Cai, S.; Tsai, R.; Tewari, M.; Minko, T.; Discher, D. E. *Nature Nanotechnol.* **2007**, *2*, 249–255.

(33) Petros, R. A.; DeSimone, J. M. *Nature Rev. Drug Discovery* **2010**, *9*, 615–627.

(34) Rzayev, J.; Hillmyer, M. A. *J. Am. Chem. Soc.* **2005**, *127*, 13373–13379.

(35) Mao, H.; Hillmyer, M. A. *Soft Matter* **2006**, *2*, 57–59.

(36) Xu, C.; Wayland, B. B.; Fryd, M.; Winey, K. I.; Composto, R. J. *Macromolecules* **2006**, *39*, 6063–6070.

(37) Xu, C.; Fu, X. F.; Fryd, M.; Xu, S.; Wayland, B. B.; Winey, K. I.; Composto, R. J. *Nano Lett.* **2006**, *6*, 282–287.

(38) Guo, F. X.; Jankova, K.; Schulte, L.; Vigild, M. E.; Ndoni, S. *Macromolecules* **2008**, *41*, 1486–1493.

(39) van Ekenstein, G. A.; Polushkin, E.; Nijland, H.; Ikkala, O.; ten Brinke, G. *Macromolecules* **2003**, *36*, 3684–3688.

(40) Keddie, J. L.; Jones, R. A. L.; Cory, R. A. *Europhys. Lett.* **1994**, *27*, 59–64.

(41) Zheng, Z. L.; Kuang, F. Y.; Zhao, J. *Macromolecules* **2010**, *43*, 3165–3168.

(42) Yu, Y. S.; Zhang, L. F.; Eisenberg, A. *Macromolecules* **1998**, *31*, 1144–1154.

(43) Suo, T. C.; Yan, D. D.; Yang, S.; Shi, A. C. *Macromolecules* **2009**, *42*, 6791–6798.